Article

Journal of
Nanoscience and Nanotechnology
Vol. 16, 6910–6918, 2016
www.aspbs.com/jnn

Drug-Loaded Carbon Nanoparticle Suspension Injection: Drug Selection, Releasing Behavior, *In Vitro* Cytotoxicity and *In Vivo* Lymph Node Targeting

Ping Xie[1], Xiaohai Tang[2, 3, *], Lei Li[3], Zhiyong Qian[4, *], Maosheng Ran[2], Xuemei Zhang[2, 3], Qian Xin[2, 3], and Haozhong Luo[2]

[1] *State Key Laboratory of Oral Diseases, West China College of Stomatology, Sichuan University, Chengdu, 610041, China*
[2] *Chongqing Lummy Pharmaceutical Co., Ltd., Chongqing, 401123, China*
[3] *College of Life Sciences, Sichuan Normal University, Chengdu, 610101, China*
[4] *State Key Laboratory of Biotherapy, West China Hospital, West China Medical School, Sichuan University, Chengdu, 610041, China*

In this study, drug-loaded carbon nanoparticle suspension as theranostic carrier was prepared for lymph node targeting delivery. Five model anti-cancer drugs were chosen to evaluate the drug selection, drug loading and releasing performance of carbon nanoparticle suspension. The relative recovery, precision, stability and limited detection range were studied in details. We found that the CNSI selectively adsorbed DOX and EPI and hardly adsorbed PTX, CDDP and 5-FU. The isothermal curves of CNSI adsorption to DOX and EPI are all fitted well with the Freundlich model. The adsorption process is not monolayer adsorption. By *in vivo* topical administration of DOX-loaded CNSI and EPI-loaded CNSI, we found that the drug-loaded CNSI were not only maintained its lymph node staining properties but also targeted delivery the drugs to the lymph node. The results demonstrated that the CNSI is not only used to vital staining of lymph vessels and lymph nodes but also can be used as drug delivery carrier. CNSI is a promising theranostic carrier for DOX or EPI delivery in cancer therapy.

Keywords: Carbon Nanoparticle, Suspension Injection, Drug Adsorption, Cytotoxicity, Lymph Node Targeting, Theranostic Carrier.

1. INTRODUCTION

Vital staining of peri-tumorous lymph vessels and lymph nodes were begun by Weinberg in 1950s.[1] Carbon black (CH40) was used for lymph mapping by Hagiwara in 1980s. While compared to methylene blue and patent blue, CH40 exhibited more specific performance in lymph mapping.[2, 3] In order to solve the poor solubility of CH40, based on CH40, carbon nanoparticle suspension injection (CNSI) has been developed in 2000s. In a prospective randomized designed multicenter clinical trial, CNSI was evaluated in intraoperative vital staining of perigastric lymph vessels and nodes before D2 lymphadenectomy.[2] It is found that the staining rate of metastatic nodes is obviously higher than that of nonmetastatic nodes, and although D2 lymph adenectomy was substantially enclosed the four main lymph drainaging directions (celiac axis, liver, mediastinum and retroperitoneum), exceptional stained nodes were pathologically identified metastasis located out of D2 region.[1] Since then, CNSI was generally applied for vital lymph staining in operative oncology in China. As the development of cancer therapy, theranostic treatment has been highlighted.[4–23] Carbon nanoparticle in CNSI is a promising drug carrier for its huge surface area.[24, 25] Combining with the lymph node targeting and mapping properties, CNSI is a potential carrier for theranostic of metastatic cancer.[26–32] However, to our knowledge, systematic research about the drug selection, drug loading and releasing performance of CNSI to the widely

*Authors to whom correspondence should be addressed.

 1533-4880/2016/16/6910/009 doi:10.1166/jnn.2016.11621

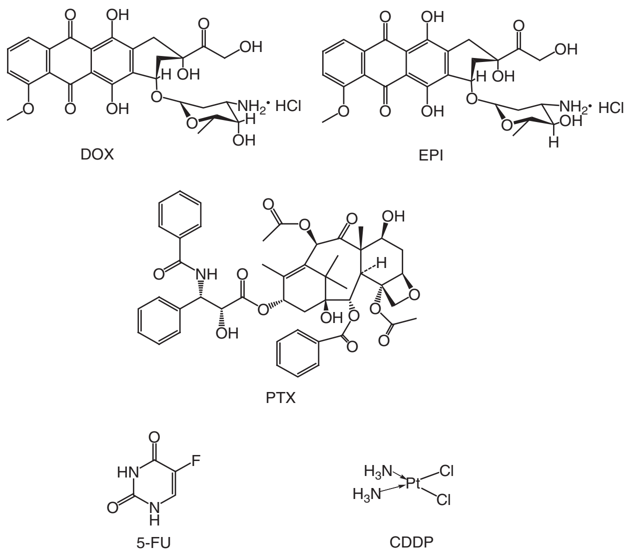

Figure 1. The chemical structures of DOX, EPI, PTX, 5-FU and CDDP.

applied chemo-drugs has not been reported.[33–37] And the lymph node targeting performance of drug-loaded CNSI is also needed to be investigated. So, in this study, kinds of model chemo-drugs, which including Doxorubicin (DOX), cis-platinum (CDDP), epirubicin (EPI), paclitaxel (PTX) and 5-fluorouracil (5-FU) (as shown in Fig. 1) were chosen to evaluate the drug selection, drug loading and releasing performance of CNSI, and the influencing factors were studied and optimized, the relative recovery, precision, stability and limited detection range were also studied in details. Furthermore, cytotoxicity of drug-loaded CNSI *in vitro* and the lymph node targeting by topical administration *in vivo* were also studied by pharmacokinetics.

2. MATERIALS AND METHODS

2.1. Materials

CNSI: Carbon nanoparticle concentration of 50 mg · mL^{-1}, marketed product, provided by Chongqing Lummy Pharmaceutical Co., Ltd (Chongqing, China). Standard substance: Doxorubicin (DOX), cis-platinum (CDDP), epirubicin (EPI), paclitaxel (PTX) and 5-fluorouracil (5-FU) were purchased from the National Institute of Control of Pharmaceutical and Biological Products (Beijing, China). Normal saline (NS), trichloromethane (THMS), methanol sodium chloride, isopropanol, sodium carbonate, sodium hydroxide and absolute ethyl alcohol, analysis of pure (AR), were purchased in Sichuan Kelong Co., Ltd., (Chengdu, China). Sodium diethyldithiocarbamatetrihydrate (DDTC) was bought in Sigma (USA). DMEM medium with high glucose, penicillin and streptomycin solution (penicillin of 10,000 units per mL concentration; streptomycin of 10,000 μg per mL concentration), and 0.25% trypsin solution were brought from Thermo Fisher Scientific (Beijing, China). Neonatal bovine serum (Shanghai Fumeng Gene Co., Ltd., Shanghai, China); PBS buffer solution (Beijing Zhongshanjinjiao Biotechnology Co., Ltd., Beijing, China); Dialysis bag (Shanghai Greenbird Co., Ltd., molecular weight cutoff 50 KDa, Shanghai, China); XB-K-25 cell counting chamber (Shanghai Qiujing Co., Ltd., Shanghai, China).

Cells: Human cancer cells line, including SiHa, HepG-2 and SKOV3, were provided by State Key Laboratory of Biotherapy of Sichuan University (Chengdu, China).

Experimental animals: Sixty New Zealand rabbits were bought from the Animal Experimental Center of Sichuan University (Chengdu, China).

2.2. Instruments

High performance liquid chromatography (HPLC), model 1260, including model G1315 DAD ultra-violet UV monitor, G1321B-1260 fluorescence detector (FLD), model G1329B auto sampler (Agilent, USA); Laser diffraction particle size analyzer, ZE-3600 (Malvern, UK); Accuracy of scales: One-hundred-thousandth gram (Mettler Toledo, Switzerland); Ultrafiltration centrifuge tube, model Amicon ultra-4 (Millipore, USA); Youpu ultrapure water system, model OPT-1-10T (Chengdu Youpu Electronics Co., Ltd., Chengdu, China); Inverted microscope (Shanghai Shunyu Co., Ltd., Shanghai, China); L-550 centrifuge (Changsha Xiangyi Centrifuge Instrument Co., Ltd., Changsha, China); Clean Bench (Suzhou Antai Airtech Co., Ltd., Suzhou, China); Carbon dioxide gas incubator (Sanyo, Japan).

2.3. Methods

2.3.1. *Optimization of Free Chem-Drugs Separation Conditions*

In the drug loading experiments, the effect of the process parameters (such as ultrafiltration tube size, centrifugation speed, centrifugation time etc.) onto the drug loading performance of CNSI have been evaluated.

2.3.1.1. Ultrafiltration Tube Size Selection. DOX solutions were prepared in three concentrations of 10, 400 and 800 μg · mL^{-1}, respectively. They were centrifugally filtered in Millipore tubes (Amicon ultra-4) of 3, 30, 50 and 100 KDa in 4000 rpm for 10 minutes, respectively. The DOX concentration of the solutions and the filtrates were measured by HPLC. This procedure was repeated for three times, and the results were expressed as mean value ± SD.

2.3.1.2. Centrifugal Speed and Time Selection. A mixture of CNSI concentration of 10 mg · mL^{-1} and DOX concentration of 2 mg · mL^{-1} was treated with ultrasonic for 5 minutes, then put in shaking bath in 37 °C, 120 rpm for 60 minutes. 2 mL of the mixture were added into Millipore tubes (Amicon ultra-4 with filter size of 50 KDa) and filtered by centrifugation with the speed of 2000 rpm for 10 minutes. Same experiments have been done except changing the speed to 3000, 4000, 5000 and 6000 rpm, respectively. The residual volumes of the mixture in upper tubes with filtrate were measured. This study

was repeated three times, and the results were expressed as mean value ± SD.

The speed of centrifugation was fixed at 4000 rpm, and the centrifugations were selected for 5, 10, 15 and 20 minutes, respectively. The residual volumes of the mixture in the upper tubes with filtrate were measured. This study was repeated three times, and the results were expressed as mean value ± SD.

2.3.2. HPLC Condition

Agilent Zorbax SB-C18 column (250 mm × 4.6 mm, 5 μm) was used; The mobile phase was sodium dodecyl sulfate (SDS) solution (1.44 g SDS and 0.68 mL phosphoric acid were dissolved in 500 mL water): acetonitrile: methanol = 500:500:60 (V/V/V); The UV detection wavelength was 254 nm; The flow rate was 1 $mL \cdot min^{-1}$; Column temperature was 25 °C and the sample size was 20 μL.

Standard curves for drugs concentration calculation were also established by HPLC via measurement of the drugs solution with different concentration.

2.3.3. Drug Loading Behavior of CNSI to DOX, EPI, PTX, 5-FU and CDDP

Model chemo-drug solutions with the same concentration (2 $mg \cdot mL^{-1}$) were prepared. DOX, EPI, 5-FU and CDDP were dissolved in PVP aqueous solution, respectively, and PTX was dissolved in anhydrous ethanol. CNSI dilutions with ten different concentrations (1, 2, 3, 4, 5, 6, 7, 8, 9 and 10 $mg \cdot mL^{-1}$, respectively) were prepared by diluting the CNSI (50 $mg \cdot mL^{-1}$) with PVP aqueous solution. The concentration of PVP aqueous solution was 20 $mg \cdot mL^{-1}$. Equal volume of drug solutions and CNSI dilutions were mixed to a final volume of 5 mL and treated with ultrasonic for 5 minutes. Then the mixture was shaded at 37 °C for 60 minutes in 120 rpm. Then the drug-adsorbed CNSI were separated by centrifugation as mentioned above. The free chemo-drug concentration in filtrate was measured by HPLC. The drug loading experiment of each model chemo-drug was performed for three times, and the results were expressed as mean value ± SD. And the percentage of drug adsorbed and the amount of drug adsorbed by per gram CNSI was calculated for further simulation.

2.3.4. Effect of Drug Concentration Onto the Particle Size of Drug-Loaded CNSI

Mixtures of CNSI and DOX were prepared by mixing the CNSI (50 $mg \cdot mL^{-1}$) and DOX aqueous solution (10 $mg \cdot mL^{-1}$) with different volume ratios. The weight ratios of CNSI and DOX were chosen as 25:0.0, 25:1.0, 25:1.5, 25:2.0 and 25:2.5 by adjusting the volume of CNSI suspension and DOX aqueous solution.

2.3.4.1. Particle Size Measurement. Particles sizes of all the mixtures were detected with Malvern particle size analyzer. Before the detection, all the mixtures were diluted by 50 times of ultra pure water. The detection was done at the time-point of 0 h and 20 h after the dilution, respectively. Each dilution was repeated for three times, and the results were expressed as mean value ± SD.

2.3.5. In Vitro Release Behavior of DOX-Loaded CNSI and EPI-Loaded CNSI

The *in vitro* release kinetics of DOX from DOX-loaded CNSI was studied by dialysis method with some modifications: DOX-loaded CNSI suspension was transferred into a dialysis bag (molecular mass cutoff is 50 KDa and the dialysis area is about 5.44 cm^2), then the dialysis bag was place into a BD tube containing 100 mL of NS. The release studying was performed at 37 °C with the shaking speed of 120 rpm. The release medium was replaced with fresh NS at predetermined time-point. The drug concentrations in the release medium were measured by HPLC. This study was repeated for three times, and the results were expressed as mean value ± SD.

Same procedure was processed in EPI-loaded CNSI.

2.3.6. Cytotoxicity of DOX-Loaded CNSI and EPI-Loaded CNSI

The cytotoxicities of cells for DOX-loaded CNSI and EPI-loaded CNSI were measured by cell counting method. Three types of cells, including SiHa, HepG-2 and SKOV3, were used to test the cytotoxicity of DOX-loaded CNSI and EPI-loaded CNSI. In brief, pretreated cells were cultured in a 12-well plate with the cell number of 2×10^4 per well. And the culturing medium was DMEM. Then the cells were incubated in an incubator (5% CO_2, 37 °C) for 24 h. Then a certain amount of DOX-loaded CNSI was added to each well. Free DOX and DMEM medium were used as the compared and negative groups, respectively. After 48 h incubation, the cell viability was measured by cell counting method. Same procedure was processed in EPI-loaded CNSI.

2.3.7. In Vivo Targeted Delivery of DOX and EPI to Lymph Node by CNSI

Sixty New Zealand rabbits were divided into four groups, which were treated with DOX intravenous injection, DOX-loaded CNSI left leg foot pad injection, EPI intravenous injection, and EPI-loaded CNSI left leg foot pad injection, respectively. The administrated dose of DOX or EPI were all fixed as 2.5 $mg \cdot kg^{-1}$.

The rabbits were sacrificed at 0.5 h, 1 h, 2 h, 3 h and 4 h after administration, respectively. In every time point, three rabbits were sacrificed for taking blood sample and popliteal lymph nodes. Blood plasma was centrifuged from the blood sample. Homogenate of lymph node was prepared by homogenizing lymph nodes according to the proportion of one gram weight of lymph node adding 10 mL of saline.

Drug extraction:Blood plasma or homogenate was treated twice for extracting DOX or EPI by adding THMS and isopropanol extract (THMS:isopropanol = 3:1, v/v). The extraction were dried and redissolved by methanol. Then, the drug concentrations in blood and lymph nodes were measured by HPLC.

3. RESULTS

3.1. Centrifugation Parameters Optimizing

3.1.1. Ultrafiltration Tube Size Selection

With a certain speed and time, the ultrafiltration tube size has some influence to the penetration of drug in centrifugation. Table I shows the concentration of DOX in the filtrate after ultrafiltration in ultrafiltration tubes with different filter sizes. It was found that most of the DOX passed through the filter while the filter sizes were larger than 50 KDa. With the consideration of the particle size of CNSI (drug carrier), Millipore tubes with filter size of 50 KDa were selected for the drug separation.

3.1.2. Centrifugal Speed and Time Determination

As shown from Tables II and III, lower centrifugal speed and less centrifugal time may cause more residual volume in upper tubes. When increasing the centrifugal speed and centrifugal time to 4000 rpm and 10 minutes respectively, residual volume changed little. For this reason, the centrifugal speed and centrifugal time were selected as 4000 rpm and 10 minutes respectively.

3.2. Drug Loading of CNSI

3.2.1. Loading Mechanism

In order to identify the dominating mechanism of the *in vitro* drug release of DOX-loaded CNSI and EPI-loaded CNSI, three kinetic models, including Langmuir, Freundlich and Temkin models, were selected to fit with the release profile.[38–41] By comparing the coefficient of correlation of each fitting curve, the one with highest R^2 value was considered as the most appropriate model. As shown from Tables IV and V, adsorption isothermal curves of CNSI adsorption to DOX and EPI fitted well with Freundlich equation, which were $\lg Qe = 0.2622 \lg Ce + 1.5587$ ($R^2 = 0.9649$) and $\lg Qe = 0.3019 \lg Ce + 1.6854$ ($R^2 = 0.9886$), respectively. CNSI has nearly no absorption to PTX, CDDP and 5-FU. Their "absorptions" to these three drugs were too low to be considered as adsorption. Tables VI~X and Figure 2 showed the drug loading performance of CNSI to DOX, EPI, PTX, 5-FU and CDDP, respectively. The results suggest that CNSI has good absorption to DOX and EPI. The CNSI hardly adsorbed PTX, 5-FU and CDDP.

Table I. The relative recovery of DOX solutions with different concentrations and filter sizes.

	Relative recovery (%)		
Filter sizes (KDa)	10 $\mu g \cdot mL^{-1}$	400 $\mu g \cdot mL^{-1}$	800 $\mu g \cdot mL^{-1}$
3	55.2 ± 0.4	54.0 ± 0.8	40.5 ± 0.5
30	96.0 ± 0.8	83.9 ± 1.1	81.4 ± 0.6
50	99.7 ± 1.3	99.5 ± 0.9	99.4 ± 0.8
100	99.6 ± 0.9	99.4 ± 1.5	99.4 ± 1.7

Table II. Determination of centrifugal speed.

Speed ($r \cdot min^{-1}$)	2000	3000	4000	5000	6000
Residual volume (mL)	0.48 ± 0.03	0.31 ± 0.02	0.26 ± 0.03	0.25 ± 0.02	0.23 ± 0.01

3.2.2. Effect of Drug Loading Onto the Particle Size of the CNSI

The relationship between the DOX dosage and the particle size of CNSI was showed in Figure 3. When the ratios of DOX:CNSI increased from 0.0 to 0.1, the particle sizes of CNSI increased from 162.0 ± 3.5 to 392.3 ± 2.9 nm, and PDI values also increased from 0.149 ± 0.015 to 0.595 ± 0.011 at 0 h, respectively; the particle sizes of the DOX-loaded CNSI further enlarged at the 20th h. It found that as the increasing of DOX dosage, the particle size of the DOX-loaded CNSI enlarged. On the other hand, the particle size of the drug-loaded particles increased either as the time increased, which suggested that the dilution was not stable.

3.3. *In Vitro* Release Behavior of Drug-Loaded CNSI

The release profile of the DOX-loaded CNSI and EPI-loaded CNSI were shown in Figure 4, respectively. Both DOX and EPI released from the CNSI were much slower than the free drug did. It indicated that the drug-loaded CNSI have the controlled release performance.[42]

3.4. Cytotoxicity of DOX-Loaded CNSI and EPI-Loaded CNSI

The effects of DOX-loaded CNSI and EPI-loaded CNSI on the vitality of SiHa, HepG-2 and SKOV3 cells were shown in Figure 5. As can be seen from the figures, DOX, DOX-loaded CNSI, EPI and EPI-loaded CNSI showed dose-dependent inhibition on SiHa, HepG-2 and SKOV3. At the same concentration, the cytotoxicties of DOX and DOX-loaded CNSI on the three tumor cells growth were no significant difference ($P > 0.05$), EPI and EPI-loaded

Table III. Determination of centrifugal time.

Time (minutes)	5	10	15	20
Residual volume (mL)	0.28 ± 0.02	0.26 ± 0.03	0.25 ± 0.01	0.25 ± 0.02

Table IV. Absorption models of DOX-loaded CNSI.

Models	Equation	Correlation coefficient
Langmuir	$1/Qe = 0.1899(1/Ce) + 0.0056$	$R^2 = 0.8077$
Freundlich	$lgQe = 0.2622lgCe + 1.5587$	$R^2 = 0.9649$
Temkin	$Qe = 88.906lgCe - 54.063$	$R^2 = 0.9061$

Notes: Qe ($mg \cdot g^{-1}$) is the average amount of adsorbed drug by CNSI; Ce ($mg \cdot L^{-1}$) is the concentration of free drug in CNSI.

Table VI. The absorption isothermal results of DOX-loaded CNSI.

CNSI:DOX	Ce ($\mu g \cdot mL^{-1}$)	Absorption rate (%)	Qe ($\mu g \cdot mg^{-1}$)
1:1	769.7 ± 3.9	23.0 ± 0.1	230.2 ± 1.8
2:1	609.5 ± 4.5	39.0 ± 0.2	195.2 ± 2.2
3:1	473.8 ± 4.0	52.6 ± 0.1	175.3 ± 1.2
4:1	335.6 ± 3.1	66.4 ± 0.2	166.0 ± 1.7
5:1	253.0 ± 5.8	74.7 ± 0.3	149.4 ± 2.5

CNSI were also the case. But the inhibition between DOX and EPI groups to these cells were difference ($P < 0.05$).

3.5. Lymph Node Targeting of Drug-Loaded CNSI *In Vivo*

Blood drug concentration and lymph node drug concentration of intravenous injection groups and topical injection groups were shown in Figure 6. It was found that DOX concentration in left leg popliteal lymph nodes of the group treated by DOX-loaded CNSI left leg foot pad injection was much higher than that of free DOX intravenous injection group. The drug concentration in the drainaging lymph nodes of the DOX-loaded CNSI treated group was 258 times higher than that of the free DOX treated group at 0.5 h. On the other hand, the blood drug concentrations of free DOX intravenous injection group were evidently higher than that of the group treated by DOX-loaded CNSI left leg foot pad injection at 0.5 h, 1 h, 2 h and 3 h, respectively. However, the blood drug concentrations of the two groups nearly reached the same at 4 h.

Similar phenomenon was found in EPI-loaded CNSI cases.

4. DISCUSSIONS

Although there were many reports about the animal studies and even clinical experiments of application of carbon nanoparticles or carbon nanotubes as carrier of chemotherapeutic agents for lymph chemotherapy,[43–45] the comprehensive and systematic methodology study about the drug loading properties of carbon nano materials has not been published. And CNSI has been widely used as a lymph tracer for vital staining drainaging lymph node of malignant tumor in operation for its huge surface area and porosity of carbon nanoparticles.[46] Therefore, in this study, CNSI was chosen as the model carbon nanobiomaterials and used as model drug carrier. Five kinds of model anticancer drugs were used to evaluate the drug selection and drug loading performance of CNSI.

Ultrafiltration has been used for the separation of free drugs and drug-loaded CNSI, instead of the methods of equilibrium dialysis and micropore filters. The driving force of ultrafiltration in separation is pressure. And ultrafiltration is a fast and efficient process in separation. However, to different separation systems, the filter size, the time and speed in centrifugation are the main factors that influencing the separation efficiency. In order to obtain perfect separation of free drug from the drug-loaded CNSI, optimizing the filter size, centrifugal speed and time in ultrafiltration is necessary.

According to the standard of Amicon ultra-4 Millipore tubes, the filter size of 3 to 100 KDa corresponds to filter size of 1 nm to 50 nm. And the average particle size of carbon nanoparticles in CNSI is about 170 nm. The sizes of the model drug are all bigger than 1 nm. So, by optimizing studying, Amicon ultra-4 Millipore tube with filter size of 50 KDa was selected as the separating device. And the centrifugal parameters were 4000 rpm in speed and 10 minutes in time. Five drugs used in this study can be quantitatively detected by HPLC method. Among them, CDDP has not the ultraviolet absorption groups so that it needs to be detected by derivation method. In this study, by literature consultation and experiments, chromatographic condition for detecting these drugs were confirmed and verified.[47–50] It has good precision and accuracy.

4.1. Drug Adsorption

From the drug-loaded results of CNSI, it is clearly found that the CNSI selectively adsorbs DOX or EPI, but exhibits no adsorption of PTX, 5-FU and CDDP. These results indicate that CNSI exhibited selectively adsorption in chemotherapeutic drugs loading. What is more important, the drug loading capacities of CNSI to DOX and EPI are up to $74.7 \pm 0.3\%$ and $91.9 \pm 1.1\%$ respectively

Table V. Absorption models of EPI-loaded CNSI.

Models	Equation	Correlation coefficient
Langmuir	$1/Qe = 0.2203(1/Ce) + 0.0028$	$R^2 = 0.9340$
Freundlich	$lgQe = 0.3019lgCe + 1.6854$	$R^2 = 0.9886$
Temkin	$Qe = 178.38lgCe - 164.37$	$R^2 = 0.9643$

Notes: Qe ($mg \cdot g^{-1}$) is the average amount of adsorbed drug by CNSI; Ce ($mg \cdot L^{-1}$) is the concentration of free drug in CNSI.

Table VII. The absorption isothermal results of EPI-loaded CNSI.

CNSI:EPI	Ce ($\mu g \cdot mL^{-1}$)	Absorption rate (%)	Qe ($\mu g \cdot mg^{-1}$)
1:1	650.3 ± 5.0	34.9 ± 0.3	349.6 ± 2.6
2:1	409.6 ± 3.2	59.0 ± 0.5	295.1 ± 2.0
3:1	257.6 ± 3.8	74.2 ± 0.8	247.4 ± 1.8
4:1	135.5 ± 4.2	86.4 ± 0.6	216.1 ± 2.3
5:1	80.4 ± 1.7	91.9 ± 1.1	183.9 ± 0.9

Table VIII. The absorption isothermal results of PTX-loaded CNSI.

CNSI:PTX	Ce ($\mu g \cdot mL^{-1}$)	Absorption rate (%)	Qe ($\mu g \cdot mg^{-1}$)
1:1	991.5 ± 8.6	0.6 ± 0.02	5.7 ± 0.2
2:1	991.5 ± 9.2	0.4 ± 0.04	3.6 ± 0.1
3:1	990.5 ± 8.0	0.4 ± 0.08	4.0 ± 0.6
4:1	990.5 ± 10.9	0.4 ± 0.05	4.0 ± 0.5
5:1	990.1 ± 9.7	0.5 ± 0.03	4.5 ± 0.3

Table X. The absorption isothermal results of CDDP-loaded CNSI.

CNSI:CDDP	Ce ($\mu g \cdot mL^{-1}$)	Absorption rate (%)	Qe ($\mu g \cdot mg^{-1}$)
1:1	944.1 ± 12.5	4.9 ± 0.2	49.4 ± 0.6
2:1	944.8 ± 10.9	4.9 ± 0.3	48.8 ± 0.8
3:1	943.4 ± 10.4	4.8 ± 0.1	48.0 ± 0.3
4:1	943.6 ± 8.8	4.8 ± 0.1	47.7 ± 0.7
5:1	943.3 ± 13.1	4.9 ± 0.2	49.3 ± 1.0

(The weight ratios of CNSI to DOX and EPI were 5:1.). The drug-loaded CNSI is a suitable nanosystem for lymph chemotherapy of commonly seen solid malignant tumors, e.g., breast cancer, gastric cancer, colorectal cancer and ovarian cancer. Furthermore, in this study, several isothermal adsorption models were used to evaluate the adsorption of CNSI to DOX and EPI. The results have shown that the adsorption of CNSI to DOX or EPI fitted well with Freundlich model. The equation of Freundlich model is $\lg Qe = \lg Kf + 1/n \times \lg Ce$, in which, Qe ($mg \cdot g^{-1}$) is the average amount of adsorbed drug by CNSI; Ce ($mg \cdot L^{-1}$) is concentration of free drug in CNSI; Kf and $1/n$ are two constants.[51] The $1/n$ value between 0.1 and 0.5 represents good adsorption of adsorbing material.[52] In the Freundlich equations of adsorption isothermal curves of DOX and EPI, the numerical value of $1/n$ are 0.2622 and 0.3019, respectively, suggesting good absorption of CNSI to the two drugs.

4.2. Adsorption Mechanism

CNSI, which is one of the allotrope of carbon, is made of SP^2 hybridized carbon atoms.[53] So there is some benzene ring in the structure of CNSI. A small amount of hydroxyl and carboxyl occur in the surface of CNSI. These groups benefit the adsorption of CNSI with drugs. It is considered that three factors involved drug adsorption mechanism of CNSI.

(1) $\pi-\pi$ stacking: Aromatic structure like anthraquinone has strong affinity for the CNSI surface due to $\pi-\pi$ stacking, so the aromatic structure the DOX or EPI tends to interact with the surface benzene ring of CNSI through $\pi-\pi$ stacking.[54] However, the other three drugs, including PTX, CDDP, 5-FU, do not have this feature.

(2) Hydrophobic interaction: There are several hydroxyl groups present in the chemical structure of DOX, EPI and PTX, thus, the –OH and –COOH functional groups of CNSI forms strong hydrogen bond with –OH or $–NH_2$ groups in the above three drugs. However, PTX is poorly soluble in water, and that hinders the adsorption with CNSI.

(3) Another possible factor that influences the drug adsorption may be the inherent cationic charge of some drugs (including DOX, EPI and CDDP).[55]

The drugs with this character may favor to adsorb to CNSI with anionic charge. CNSI exhibited poor adsorption capacity to 5-FU or PTX may be ascribe to the neutral structure of 5-FU or PTX. By the combined actions of all these three forces, CNSI selectively adsorbed DOX or EPI.

Table IX. The absorption isothermal results of 5-FU-loaded CNSI.

CNSI:5-FU	Ce ($\mu g \cdot mL^{-1}$)	Absorption rate (%)	Qe ($\mu g \cdot mg^{-1}$)
1:1	991.5 ± 10.8	0.2 ± 0.01	2.1 ± 0.1
2:1	991.7 ± 12.7	0.4 ± 0.03	3.5 ± 0.1
3:1	992.3 ± 13.0	0.3 ± 0.02	3.0 ± 0.2
4:1	992.0 ± 9.2	0.3 ± 0.05	2.9 ± 0.2
5:1	990.0 ± 15.3	0.4 ± 0.07	3.6 ± 0.3

4.3. Particle Size Related to Lymph Targeting

The average particle size of CNSI is about 170 nm. It is designed to be rapid and targeted flowing in the drainaging lymph capillaries and the lymph nodes near the injected site. This is the basic property of CNSI for vital staining of drainaging lymph nodes of malignant tumor during operation.

However, using as a carrier of chemotherapeutic agents for targeting lymph chemotherapy, the particle size of the drug-loaded CNSI needs not to be smaller than 200 nm. Lymph capillary originates from caecum in tissue. They connect with each other to form a lymph network, and feed

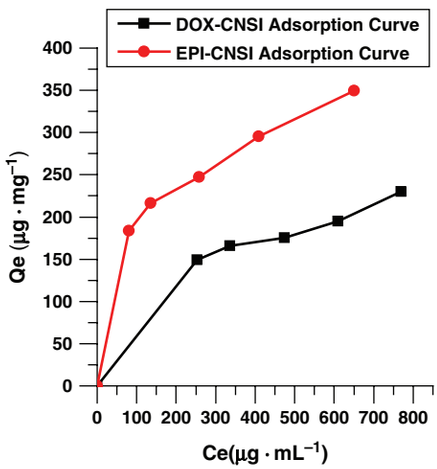

Figure 2. The absorption isothermal curves of DOX-loaded CNSI and EPI-loaded CNSI. Results showed that the CNSI to DOX and EPI has good adsorption, and simulation of the Freundlich isothermal adsorption equations were $\lg Qe = 0.2622 \lg Ce + 1.5587$ ($R^2 = 0.9649$) and $\lg Qe = 0.3019 \lg Ce + 1.6854$ ($R^2 = 0.9886$), respectively.

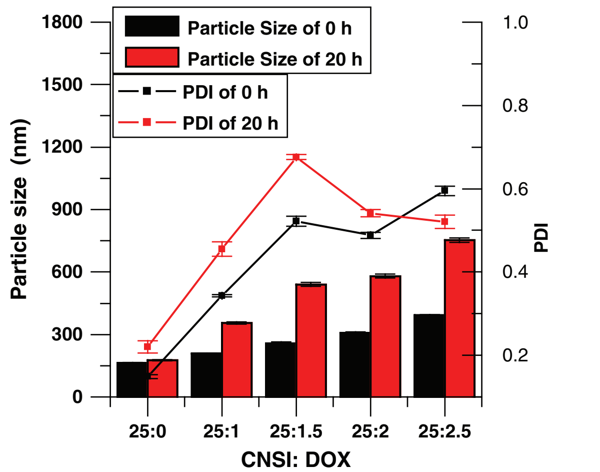

Figure 3. Particle size was influenced by the DOX proportion in the CNSI and DOX mixture. As shown from Figure 3, it found that as the increasing of DOX dosage, the particle size of the CNSI enlarged. The particle size of CNSI and DOX mixture magnified as the proportion of DOX in the mixture increased.

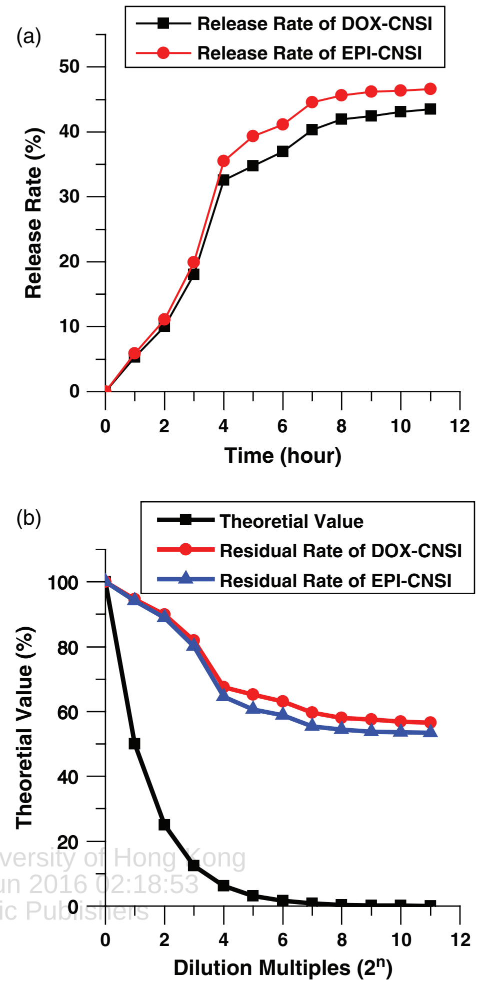

Figure 4. (a) The release rate of DOX-loaded CNSI and EPI-loaded CNSI in different time. (b) The free DOX and EPI residual rate of DOX-loaded CNSI and EPI-loaded CNSI with different dilution multiples. Results showed that the release rate of DOX-loaded CNSI and EPI-loaded CNSI were at about 43% and 46%, respectively. The release rate increased along with the increase of release medium volume, but the adsorption of DOX or EPI in the preparation did not completely released. Results of the free DOX or EPI concentration in the solution showed that the DOX-loaded CNSI or EPI-loaded CNSI slow-release effect can keep for a long time in the body above the minimum concentration of tumor suppression.

into lymph vessels.[56] Lymph capillary has the structure of large and irregular lumen, thin wall which is comprised only by the endothelial and extremely thin connective tissue and without epithelial cells. Under the electron microscope, endothelial cells of lymph capillary have large gap,[57] without basal membrane which appear high permeability for easy enter of macromolecular, cells and bacteria. The inner diameter of capital lymph capillary of tumor drainaging area varied from 200 nm to more than 800 nm according to the pathological physiological function.[58] Therefore, the particle size of the drug-loaded CNSI is not necessary to be less than 200 nm. If the lymph chemotherapy administrated one to two days before the operation, there is enough time for CNSI to go through the lymph vessels and nodes from the injected site.

4.4. Drug Releasing Behaviors of Drug-Loaded CNSI

The accumulated release of both DOX and EPI are all trend to equilibrium in 8 h from the beginning of drug releasing experiment. The accumulated release drugs from DOX-loaded CNSI and EPI-loaded CNSI are about 43% and 46% at the 8th h, respectively. The release rate increased along with the increase of release medium volume, but quite amount of DOX and EPI adsorbed onto carbon nanoparticles released much slower after 8 h. The results demonstrated that the drug-loaded CNSI has the long-term drug releasing performance.

4.5. Cytotoxicity of DOX-Loaded CNSI and EPI-Loaded CNSI

In cytotoxic experiments, the culture medium was stained dark by carbon nanoparticles of CNSI, and they could not be eliminated completely. It indicates that the cell viability cannot be measured by the optical detection manner, such as CCK8 or MTT. Therefore, artificial cell counting was adopted in the study to overcome the above problem. The result of cytotoxic experiment suggests that DOX-loaded CNSI can effectively inhibit cancer cells growth. And EPI-loaded CNSI has the similar results. This is the key point that DOX-loaded CNSI and EPI-loaded CNSI have potential properties to be developed to a lymph targeting anticancer agent.

4.6. Lymph Node Targeting of Drug-Loaded CNSI

In intravenous application, it is a challenge to efficiently deliver DOX or EPI to lymph nodes. It is not conducive

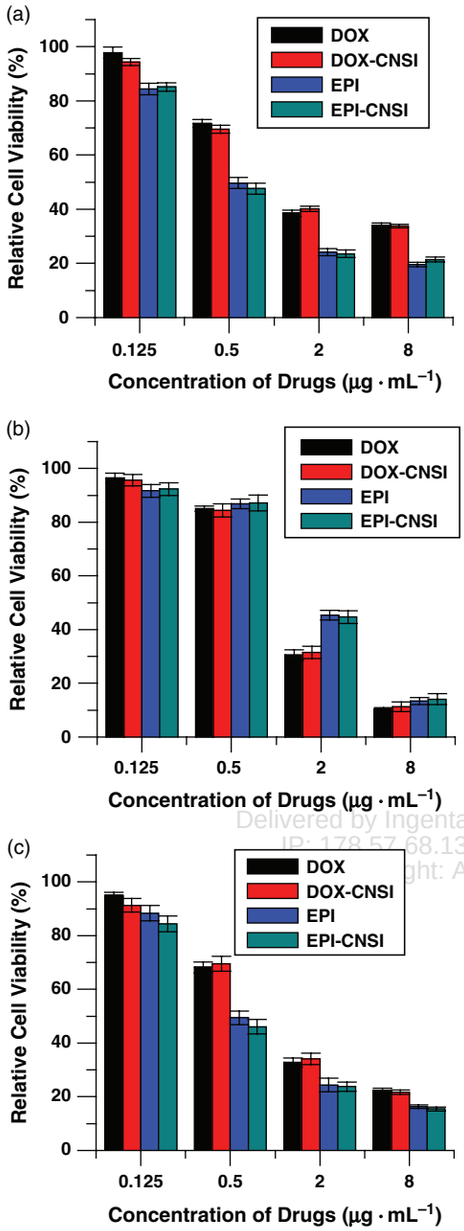

Figure 5. Cytotoxicity of DOX, DOX-loaded CNSI, EPI and EPI-loaded CNSI against (a) HepG-2 liver carcinoma cells, (b) SiHa cervix carcinoma cells, and (c) SKOV3 ovary cancer cells. These drugs were treated in a 12 well plate with 2×10^4 cells/well for 2 days.

to obtain sufficient chemotherapeutic effect in lymph metastasis inhibition, which is common in solid cancers. In this study, it was found that topical injection of drug-loaded CNSI can obviously increase the drug concentration in the drainaging lymph nodes compare to that of intravenous administration. This result suggests that drug-loaded CNSI are potential candidates in treatment of lymph metastasis by topical administration.

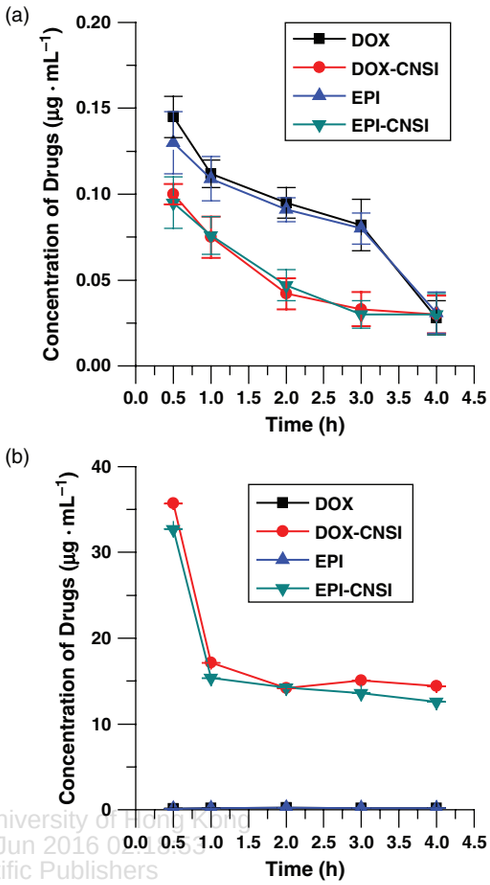

Figure 6. Blood drug concentration-time curves (a) and lymph node drug concentration-time curves (b) in DOX intravenous injection group, DOX-loaded CNSI left leg foot pad injection group, EPI intravenous injection group and EPI-loaded CNSI left leg foot pad injection group, respectively.

5. CONCLUSIONS

In conclusion, CNSI selectively adsorbed DOX and EPI. And the drug-loaded CNSI exhibited controlled drug release behavior. The DOX-loaded CNSI and EPI-loaded CNSI can effectively suppressed the growth of several kinds of cancer cells. And DOX-loaded CNSI and EPI-loaded CNSI can gather DOX and EPI in the drainaging lymph nodes when they are topically applied. The results demonstrate that the DOX-loaded CNSI or EPI-loaded CNSI are the suitable and promising candidates for lymph targeting chemotherapy.

Acknowledgments: This study was partly supported by the major drug discovery science and technology major projects of 12th five-year national plan and research fund for major drug research of Nation Science and Technology (863 Project, 2012ZX09102-101-015, 2012-2015 0/446.64).

References and Notes

1. J. Weinberg and E. M. Greaney, *Surg. Gynecol. Obstet.* 90, 561 (**1950**).
2. S. K. Nune, P. Gunda, B. K. Majeti, P. K. Thallapally, and M. L. Forrest, *Adv. Drug Deliver. Rev.* 63, 882 (**2011**).
3. M. Q. Chu, J. L. Peng, J. J. Zhao, S. L. Liang, Y. X. Shao, and Q. Wu, *Biomaterials* 34, 1820 (**2013**).
4. L. M. Zhang, Z. L. Wang, Z. X. Lu, H. Shen, J. Huang, M. Liu, N. Y. He, and Z. J. Zhang, *J. Mater. Chem. B* 1, 749 (**2013**).
5. N. Paitya, *J. Bionanosci.* 7, 145 (**2013**).
6. L. M. Zhang, Z. X. Lu, Y. Y. Bai, T. Wang, Z. F. Wang, J. Chen, Y. Ding, F. Yang, Z. D. Xiao, S. H. Ju, J. J. Zhu, and N. Y. He, *J. Mater. Chem. B* 1, 1289 (**2013**).
7. A. K. Babahedari, E. H. Soureshjani, M. K. Shamsabadi, and H. Kabiri, *J. Bionanosci.* 7, 288 (**2013**).
8. X. Y. Ji, W. J. Yang, T. Wang, C. Mao, L. L. Guo, J. Q. Xiao, and N. Y. He, *J. Biomed. Nanotechnol.* 9, 1672 (**2013**).
9. L. Jin, X. Zeng, M. Liu, and N. Y. He, *Sci. Adv. Mater.* 5, 2053 (**2013**).
10. G. Amsaveni, A. S. Farook, V. Haribabu, R. Murugesan, and A. Girigoswami, *Adv. Sci. Eng. Med.* 5, 1340 (**2013**).
11. T. Wang, Y. Hu, M. K. Leach, L. Zhang, W. J. Yang, L. Jiang, Z. Q. Feng, and N. Y. He, *Int. J. Pharm.* 422, 462 (**2012**).
12. L. M. Zhang, Z. X. Lu, X. L. Li, Y. Deng, F. Q. Zhang, C. Ma, and N. Y. He, *Polym. Chem.* 3, 1958 (**2012**).
13. N. Gupta, A. Panwar, R. Kumar, S. K. Sharma, R. K. Sharma, and V. Agrawal, *Adv. Sci. Eng. Med.* 5, 355 (**2013**).
14. T. Wang, L. J. Xu, S. Li, and N. Y. He, *Low Mol. Nanoscale* 2, 230 (**2010**).
15. J. Fu, D. X. Wang, T. Wang, W. J. Yang, Y. Deng, H. Wang, S. G. Jin, and N. Y. He, *J. Biomed. Nanotechnol.* 6, 725 (**2010**).
16. W. J. Yan, T. Wang, and N. Y. He, *Chem. J. Chinese U* 30, 625 (**2009**).
17. W. J. Yang, T. Wang, J. Fu, and N. Y. He, *J. Biomed. Nanotechnol.* 5, 591 (**2009**).
18. T. Wang, Z. Q. Feng, N. Y. He, Z. F. Wang, S. Li, Y. F. Guo, and L. J. Xu, *J. Nanosci. Nanotechnol.* 7, 4571 (**2007**).
19. K. Ilango, T. M. Vijayakumar, A. Agrawal, and G. P. Dubey, *J. Bionanosci.* 7, 127 (**2013**).
20. A. Mujtaba, K. Kohli, J. Ali, and S. Baboota, *Adv. Sci. Eng. Med.* 5, 349 (**2013**).
21. S. Amin, A. Sarfenejad, J. Ahmad, K. Kohli, and S. R. Mir, *Adv. Sci. Eng. Med.* 5, 299 (**2013**).
22. M. M. Varma, V. Sravani, and P. V. Swamy, *J. Bionanosci.* 7, 560 (**2013**).
23. M. M. Varma, A. L. Harika, and V. Sravani, *J. Bionanosci.* 7, 360 (**2013**).
24. F. Guo, X. Mao, J. Wang, F. Luo, and Z. Wang, *J. Inter. Med. Res.* 39, 2217 (**2011**).
25. B. S. Wong, S. L. Yoong, A. Jagusiak, T. Panczyk, H. K. Ho, W. H. Ang, and G. Pastorin, *Adv. Drug Deliv. Rev.* 65, 1964 (**2013**).
26. S. P. Egusquiaguirre, M. Igartua, R. M. Hernandez, and J. L. Pedraz, *Clin. Transl. Oncol.* 2, 83 (**2012**).
27. N. N. Ma, C. Ma, C. Y. Li, T. Wang, Y. J. Tang, H. Y. Wang, X. B. Mou, Z. Chen, and N. Y. He, *J. Nanosci. Nanotechnol.* 13, 6485 (**2013**).
28. J. Xie, S. Lee, and X. Y. Chen, *Adv. Drug Deliv. Rev.* 62, 1065 (**2010**).
29. F. Yang, C. Jin, S. Subedi, C. L. Lee, Q. Wang, Y. Jiang, J. Li, Y. Di, and D. L. Fu, *Cancer Treat. Rev.* 38, 566 (**2012**).
30. T. Yokota, T. Saito, Y. Narushima, K. Iwamoto, M. Iizuka, A. Hagiwara, K. Sawai, S. Kikuchi, Y. Kunii, and H. Yamauchi, *Can. J. Surg.* 43, 191 (**2000**).
31. A. Cousins, S. K. Thompson, A. B. Wedding, and B. Thierry, *Biotechnol. Adv.* 32, 271 (**2014**).
32. H. A. Schreiber, J. Prechl, H. Q. Jiang, A. Zozulya, Z. Fabry, F. Denes, and M. Sandor, *J. Immunol. Methods* 356, 47 (**2010**).
33. T. Muthukumar, S. Prabhavathi, M. Chamundeeswari, and T. P. Sastry, *Mater. Sci. Eng. C Mater. Biol. Appl.* 36, 14 (**2014**).
34. N. I. Ma, C. Ma, Y. Deng, T. Wang, and N. Y. He, *J. Nanosci. Nanotechnol.* 13, 3 (**2013**).
35. R. Zhang and H. Olin, *Mater. Sci. Eng. C* 32, 1247 (**2012**).
36. H. R. Qian, J. Fan, and Y. B. Liu, *J. Practical Oncol.* 21, 146 (**2006**).
37. L. Jin, X. Zeng, M. Liu, Y. Deng, and N. Y. He, *Theranostics* 4, 241 (**2014**).
38. I. A. W. Tan, A. L. Ahmad, and B. H. Hameed, *J. Hazardous Mater.* 164, 473 (**2009**).
39. O. Hamdaouianad and E. Naffrechoux, *J. Hazardous Mater.* 147, 381 (**2007**).
40. Z. K. George, K. L. Nikolaos, and A. D. Eleni, *Chem. Eng. J.* 234, 491 (**2013**).
41. L. Ren, J. Zhang, Y. Li, and C. Li, *Chem. Eng. J.* 168, 553 (**2011**).
42. X. K. Zhang, L. J. Meng, Q. H. Lu, Z. F. Fei, and P. J. Dyson, *Biomaterials* 30, 6044 (**2009**).
43. Z. Liu, X. Sun, N. N. Ratchford, and H. Dai, *ACS Nano* 1, 51 (**2007**).
44. T. Murakam, K. Ajima, J. Miyawaki, M. Yudasaka, S. Iijima, and K. Shiba, *Mol. Pharm.* 6, 399 (**2004**).
45. G. Q. Lu, J. Yan, and G. Li, *Chin. J. Lab. Diagn.* 11, 1994 (**2012**).
46. Y. Gao, J. J. Xie, H. J. Chen, S. G. Gu, R. L. Zhao, J. W. Shao, and L. Jia, *Biotechnol. Adv.* 32, 764 (**2014**).
47. J. C. Pionteka, A. J. Skaa, M. Zajac, M. Sobczaka, A. Bartolda, and I. Oszczapowicz, *J. Pharm. Biomed. Anal.* 50, 576 (**2009**).
48. S. R. Datir, M. Das, R. P. Singh, and S. Jain, *Bioconjug. Chem.* 23, 2202 (**2012**).
49. C. F. Chin, Q. Tian, M. I. Setyawati, W. Fang, E. S. Tan, D. T. Leong, and W. H. Ang, *J. Med. Chem.* 55, 7572 (**2012**).
50. Y. Li, Y. Liu, Y. J. Fu, T. T. Wei, L. L. Guyader, G. Gao, R. S. Liu, Y. Z. Chang, and C. Y. Chen, *Biomaterials* 33, 403 (**2012**).
51. W. S. Wanngah, L. C. Teong, R. H. Toh, and M. A. K. M. Hanafiah, *Chem. Eeng. J.* 15, 46 (**2012**).
52. O. Hamdaoui and E. Naffrechoux, *J. Hazardous Mater.* 147, 387 (**2007**).
53. E. Heister, V. Neves, C. Lamprecht, S. R. P. Silva, H. M. Coley, and J. McFadden, *Carbon* 50, 623 (**2012**).
54. H. Liu, H. Xu, Y. Wang, Z. He, and S. Li, *Drug Dev. Ind. Pharm.* 38, 1032 (**2012**).
55. S. R. Datir, M. Das, R. P. Singh, and S. Jain, *Bioconjug. Chem.* 23, 2202 (**2012**).
56. K. M. Honkonen, M. T. Visuri, T. V. Tervala, P. J. Halonen, M. B. Koivisto, M. T. Lahteenvuo, K. K. Alitalo, S. Y. Herttuala, and A. M. Saaristo, *Ann. Surg.* 5, 962 (**2013**).
57. H. Nehoff, N. N. Parayath, L. Domanovitch, S. Taurin, and K. Greish, *Int. J. Nanomed.* 9, 2539 (**2014**).
58. S. M. Moghimi, A. C. Hunter, and J. C. Murray, *Pharmacol. Rev.* 53, 286 (**2001**).

Received: 12 May 2014. Accepted: 18 July 2014.